Geophys. J. Int. (1996) **124,** 113–120

Depth estimation from the scaling power spectrum of potential fields?

Stefan Maus and Vijay Dimri
National Geophysical Research Institute, Hyderabad 500 007, India

Accepted 1995 July 22. Received 1995 July 20; in original form 1994 May 3

SUMMARY

Depth estimation from potential field power spectra requires a realistic assumption of the statistical properties of the source distributions. Density and susceptibility distributions in the Earth's crust exhibit a long-range dependence, which is adequately described by *scaling* random fields with a spectral density proportional to some power of the wavenumber. The theoretical power spectrum for a half-space model of scaling sources explains the shape of observed power spectra of real potential field data very well. Minimizing the misfit between the model and the observed power spectrum yields an estimate for the depth to the top of the sources. After demonstrating this approach on synthetic magnetic data, we reinterpret power spectra of gravity and aeromagnetic data from Utah, Hawaii and Saskatchewan, finding depth values that differ significantly from earlier interpretations. All three power spectra are best explained by source distributions starting at surface level, even the power spectrum from an aeromagnetic survey of a sedimentary basin with virtually non-magnetic basin fill. In the latter case, *a priori* information on the intensity and the scaling exponent of the field caused by the basement had to be included to obtain an approximate estimate of the basin depth. In general, potential field power spectra are dominated by scaling properties of their source distributions and contain only limited depth information.

Key words: fractals, gravity anomalies, magnetic anomalies, spectral analysis.

INTRODUCTION

Spectral analysis of gravity and magnetic data has been used extensively during the past two decades to derive the depth to certain geological features, such as the magnetic basement (e.g. Spector & Grant 1970; Hahn, Kind & Mishra 1976; Connard, Couch & Gemperle 1983; Bosum *et al.* 1989; Pederson 1991; Garcia-Abdeslem & Ness 1994) or the Curie-temperature isotherm (e.g. Shuey *et al.* 1977; Blakely 1988; Okubo & Matsunaga 1994).

Spector & Grant (1970) stated that the depth factor invariably dominates the shape of the radially averaged power spectrum of magnetic data. Here, 'radially averaged' means that the powers for equal lengths of the wavevector are averaged. This statement has paved the way for a very convenient interpretation of the power spectrum of potential field data. The radially averaged power spectrum of the field in a 2-D observation plane decreases with increasing depth to source t by a factor $\exp(-2tr)$, r being the wavenumber. Hence, if the depth factor dominates the shape of the power spectrum, the logarithm of the power spectrum should be proportional to $-2tr$, and the depth to source can be derived directly from the slope of the log radially averaged power spectrum. Since the latter is usually curved, a single power spectrum may yield up to five depth values (Connard *et al.* 1983), which seems to indicate the existence of various horizontal magnetic interfaces in the crust. The same line of reasoning can be applied to gravity power spectra, yielding a method for depth estimation from gravity data. In the following, we will refer to both of these methods as the 'Spector and Grant method', although Spector and Grant proposed their method only for the interpretation of *aeromagnetic* data. Various theories have been proposed to justify Spector and Grant's approach. We give a brief, critical review of these theories in the second section of this paper.

A reasonable model for depth estimation has to explain the shape of the log power spectrum, which is not a straight line. Furthermore, the assumptions on the source distributions have to be realistic. Pilkington & Todoeschuck (1990) pointed out that the concept of scaling noises (Mandelbrot 1983) is appropriate for modelling the spatial variation of many geophysical parameters, such as the density in the Earth's crust. Scaling noises are random functions with a power spectral density proportional to $s^{-\beta}$, where s is the absolute value of the wavevector and β is referred to as the scaling exponent. The first application of this concept to magnetic fields was made by Gregotski, Jensen & Arkani-Hamed (1991), who studied scaling properties of aeromagnetic surveys of the North American continent to derive a deconvolution operator for susceptibility mapping. The power spectrum of the aeromagnetic map of South Africa, derived by Whaler (1994), shows that magnetic fields can have scaling properties up to wavelengths of at least several hundred kilometres. Pilkington & Todoeschuck (1993, 1995) confirmed scaling properties of the susceptibility distribution in the crust on susceptibility logs and on surface susceptibility measurements. Using a formula of Naidu (1968), they derived a relationship between the scaling exponent of the 3-D susceptibility distribution in the crust and the 2-D magnetic field in a horizontal observation plane. Further relationships between scaling exponents of potential fields and their sources for various cross-sections are given by Maus & Dimri (1994).

In this paper, we derive the theoretical power spectrum of the gravity and magnetic fields for a half-space of sources with an isotropic scaling exponent. This model power spectrum is first compared with the power spectrum of synthetic magnetic data. Then we use the model power spectrum to reinterpret a gravity and two aeromagnetic power spectra from the literature.

We follow Turcotte (1992) and denote the scaling exponent of a source distribution with β. The scaling exponent of the field is referred to as γ. Whenever we refer to the magnetic field and the gravity field, we mean the anomaly of the total intensity of the magnetic field and the anomaly of the vertical gradient of the gravity potential, respectively.

THE SPECTOR AND GRANT METHOD

Spector & Grant (1970) approximated the susceptibility distribution in the space domain by a number of rectangular prisms. They derived a model power spectrum which includes a factor for the horizontal susceptibility variations and a depth factor $\exp(-2\bar{h}r)$, where $\bar{h}$ is the mean depth to the top of the prisms and r is the absolute value of the wavevector. Stating that 'The $e^{-2\bar{h}r}$-term is invariably the dominating factor in the power spectrum', Spector & Grant introduced a method that estimates the depth to source directly from the slope of the log radially averaged power spectrum. This method enjoys continuing popularity, as can be seen from a number of recent publications (e.g. Ofoegbu & Hein 1991; Cowan & Cowan 1993; Hildenbrand, Rosenbaum & Kauahikaua 1993). An example of an interpretation by the Spector and Grant method is shown in Fig. 4 (after Hildenbrand *et al.* 1993).

The prism approach of Spector and Grant leads to a power spectrum which includes factors other than the depth to source. However, Naidu (1972) pointed out a model for which the power spectrum consists *only* of the depth factor. It is a half-space consisting of a white noise of semi-infinite needles with constant magnetization. A modification of this model was proposed by Hahn *et al.* (1976), who substituted the semi-infinite needles by slim prisms with a finite depth extent of the order of magnitude of the grid size. Furthermore, a positive autocorrelation in the susceptibility of the prisms was assumed. This model accounts for strong horizontal susceptibility variations but assumes a constant susceptibility in the vertical direction.

The Spector and Grant method can also be applied to the power spectrum of gravity data. Pawlowski (1994, 1995) assumes a density equivalent layer of white noise at a certain depth. Using a formula of Naidu (1968), he shows that this equivalent layer causes a gravity field, with the slope of its log power spectrum being proportional to the depth of the layer. A shortcoming of this method is that it only yields the depth to the equivalent layer and not the depth to the real sources, which may be situated anywhere above or below this layer.

Spector and Grant's understanding of the power spectrum has another widespread application. If the slope of the log power spectrum indicates the depth to source, then a section with constant slope defines a spectral band of the potential field originating from sources of equal depth. Hence, it appears to be possible to separate the contribution of these particular sources from the rest of the field by band-pass filtering (Spector & Grant 1970; Jacobsen 1987; Cowan & Cowan 1993; Pawlowski 1994, 1995). Since the low-wavenumber (long-wavelength) portion of the power spectrum is usually rather steep (e.g. Figs 2, 4, 7 and 8), this implies that long-wavelength anomalies necessarily originate from deep-seated sources. However, a magnetic anomaly of large areal extent may also be due to a large, weakly magnetized shallow structure (d'Arnaud Gerkens 1989, p. 483), and the regional gravity field may very well be caused by shallow structures, such as extensive sedimentary basins (i.e. Militzer & Weber 1984, p. 229).

THEORY

In the following, we derive the spectral density of the gravity and magnetic fields in an observation plane located at a distance t above a half-space of sources. The source distribution is modelled by a random function with scaling properties. To express the spectral properties of these random functions we utilize the Fourier–Stieltjes integral for homogeneous random fields as described by Yaglom (1986, pp. 322–390).

Homogeneous random fields

The 3-D source distributions and their respective fields can be considered as random functions of the spatial coordinates $\mathbf{r} = (x, y, z)$. A scalar random function of more than one parameter is called a *random field*. A random field $X(\mathbf{r})$ is said to be *homogeneous in a wide sense*, if its mean value is constant and its correlation function $B(\mathbf{r}_1, \mathbf{r}_2) = \langle X(\mathbf{r}_1)X(\mathbf{r}_2)\rangle$ depends only on the vector $(\mathbf{r}_1 - \mathbf{r}_2)$. Here, $\langle . \rangle$ denotes mathematical expectation. Furthermore, a homogeneous random field is called isotropic, if its correlation function depends only on the *length* of the vector $(\mathbf{r}_1 - \mathbf{r}_2)$. A 3-D homogeneous random field $X(\mathbf{r})$ can be written as a Fourier–Stieltjes integral over the wavenumber domain R^3 as

$$X(\mathbf{r}) = \int_{R^3} e^{i\mathbf{k}\cdot\mathbf{r}} Z(d\mathbf{k}), \tag{1}$$

where $d\mathbf{k} \in R^3$ is a 3-D interval in the wavenumber domain, $Z(d\mathbf{k})$ is a complex random measure determined for any such interval $d\mathbf{k}$ and having the following properties:

(1) $\langle Z(d\mathbf{k})\rangle = 0$ for all intervals $d\mathbf{k}$;

(2) $\langle Z(d\mathbf{k})\overline{Z(d\mathbf{k}')}\rangle = 0$ if the intervals $d\mathbf{k}$ and $d\mathbf{k}'$ are non-intersecting;

(3) $Z(d\mathbf{k} \cup d\mathbf{k}') = Z(d\mathbf{k}) + Z(d\mathbf{k}')$ if the intervals $d\mathbf{k}$ and $d\mathbf{k}'$ are non-intersecting.

If a spectral density f(**k**) exists for that random field, it is related to $Z(d\mathbf{k})$ by

$$\langle |Z(d\mathbf{k})|^2 \rangle = f(\mathbf{k})\, du\, dv\, dw, \tag{2}$$

where $\mathbf{k} = (u, v, w)$. Combining (2) with the independence of the random measure (property 2) gives a single symbolic relation:

$$\langle Z(d\mathbf{k})\overline{Z(d\mathbf{k}')} \rangle = \delta(\mathbf{k} - \mathbf{k}') f(\mathbf{k})\, du\, dv\, dw\, du'\, dv'\, dw', \tag{3}$$

where $\delta(\mathbf{k})$ is the Dirac delta function.

The integral of (1) is evaluated in a somewhat different way from the conventional Riemann integral. The wavenumber domain R^3 is divided into small intervals $d\mathbf{k}$. For each interval we have a complex random number Z, hence $Z(d\mathbf{k})$. Each interval is also associated with a value of the wavevector $\mathbf{k}$. We evaluate $\exp(i\mathbf{k}\cdot\mathbf{r})$ for this value of $\mathbf{k}$ and the fixed value of $\mathbf{r}$. Then we multiply the result by the complex random number $Z(d\mathbf{k})$. Summing over all intervals $d\mathbf{k}$ we obtain the value of the Fourier–Stieltjes integral.

In the following, we shall assume that the source distributions as well as their respective fields are homogeneous random fields which can be written as Fourier–Stieltjes integrals. This enables us to derive a relationship between the spectral density of a source distribution and its respective field for the gravity as well as the magnetic case.

Spectrum of the 3-D gravity field

Inside an anomalous density distribution $\rho(\mathbf{r})$, the potential $V(\mathbf{r})$ of the anomalous gravity field satisfies Poisson's equation,

$$\Delta V(\mathbf{r}) = C_\rho \rho(\mathbf{r}), \tag{4}$$

where C_ρ is a constant. Considering the vertical gradient $g(\mathbf{r}) = \delta V(\mathbf{r})/\delta z$ we get

$$\Delta g(\mathbf{r}) = C_\rho \frac{\delta}{\delta z} \rho(\mathbf{r}). \tag{5}$$

Expressing $g(\mathbf{r})$ and $\rho(\mathbf{r})$ as Fourier–Stieltjes integrals leads to

$$\Delta \int_{R^3} \exp(i\mathbf{k}\cdot\mathbf{r}) Z_g(d\mathbf{k}) = C_\rho \frac{\delta}{\delta z} \int_{R^3} \exp(i\mathbf{k}\cdot\mathbf{r}) Z_\rho(d\mathbf{k}),$$

$$-\int_{R^3} |\mathbf{k}|^2 \exp(i\mathbf{k}\cdot\mathbf{r}) Z_g(d\mathbf{k}) = C_\rho \int_{R^3} iw \exp(i\mathbf{k}\cdot\mathbf{r}) Z_\rho(d\mathbf{k}), \tag{6}$$

where w is the z-component of the wavevector and Z_g and Z_ρ are the random measures in the wavenumber domain for the gravity field and the density distribution, respectively. Multiplying by the complex conjugates on both sides of eq. (6) and using eq. (3) yields

$$\int_{R^3}\int_{R^3} |\mathbf{k}|^2 |\mathbf{k}'|^2 \exp(i\mathbf{k}\cdot\mathbf{r})\, \overline{\exp(i\mathbf{k}'\cdot\mathbf{r})} Z_g(d\mathbf{k}) \overline{Z_g(d\mathbf{k}')}$$

$$= C_\rho^2 \int_{R^3}\int_{R^3} iw\overline{iw'} \exp(i\mathbf{k}\cdot\mathbf{r})\, \overline{\exp(i\mathbf{k}'\cdot\mathbf{r})} Z_\rho(d\mathbf{k}) \overline{Z_\rho(d\mathbf{k}')}$$

$$\int_{R^3}\int_{R^3} |\mathbf{k}|^2 |\mathbf{k}'|^2 \exp(i\mathbf{k}\cdot\mathbf{r})$$

$$\times \exp(-i\mathbf{k}'\cdot\mathbf{r}) \delta(\mathbf{k} - \mathbf{k}') f_g(\mathbf{k})\, du\, dv\, dw\, du'\, dv'\, dw'$$

$$= C_\rho^2 \int_{R^3}\int_{R^3} ww' \exp(i\mathbf{k}\cdot\mathbf{r})$$

$$\times \exp(-i\mathbf{k}'\cdot\mathbf{r}) \delta(\mathbf{k} - \mathbf{k}') f_\rho(\mathbf{k})\, du\, dv\, dw\, du'\, dv'\, dw'$$

$$\int_{R^3} |\mathbf{k}|^4 f_g(\mathbf{k})\, du\, dv\, dw = C_\rho^2 \int_{R^3} w^2 f_\rho(\mathbf{k})\, du\, dv\, dw. \tag{7}$$

Consequently, the spectral density of f_g of the gravity field is related to the spectral density f_ρ of the density distribution by

$$f_g(\mathbf{k}) = C_\rho^2 \frac{w^2}{|\mathbf{k}|^4} f_\rho(\mathbf{k}). \tag{8}$$

Spectrum of the 3-D magnetic field

A similar equation can be derived for the magnetic field (Maus & Dimri 1994), relating the spectral density f_χ of the susceptibility distribution to the spectral density f_T of the anomaly of the total intensity of the magnetic field reduced to the pole by

$$f_T(\mathbf{k}) = C_\chi^2 \frac{w^4}{|\mathbf{k}|^4} f_\chi(\mathbf{k}), \tag{9}$$

where C_χ is a constant.

Spectra of the 2-D potential fields in the xy-plane

Since we cannot observe the field in three dimensions, we will now derive the spectral densities for a horizontal observation plane at $z = 0$. The gravity field, $g(x, y, 0)$, can then be written as a Fourier–Stieltjes integral:

$$\begin{aligned} g(x, y, 0) &= \int_{R^3} \exp[i(ux + vy + 0w)] Z^{3\text{-D}}(d\mathbf{k}) \\ &= \int_{R^2} \exp[i(ux + vy)] \int_R Z^{3\text{-D}}(du\, dv\, dw) \\ &= \int_{R^2} \exp[i(ux + vy)] Z^{2\text{-D}}(du\, dv), \end{aligned} \tag{10}$$

where

$$Z^{2\text{-D}}(du\, dv) = \int_R Z^{3\text{-D}}(du\, dv\, dw).$$

Using the eqs (2) and (3), we can relate the 2-D spectral density $f^{2\text{-D}}$ in the observation plane to the 3-D spectral density $f^{3\text{-D}}$ of the field by

$$\begin{aligned} f^{2\text{-D}}(u, v) &= \langle |Z^{2\text{-D}}(du\, dv)|^2 \rangle \\ &= \left\langle \left| \int_R Z^{3\text{-D}}(du\, dv\, dw) \right|^2 \right\rangle \\ &= \left\langle \int_R \int_R Z^{3\text{-D}}(du\, dv\, dw) \overline{Z^{3\text{-D}}(du\, dv\, dw')} \right\rangle \\ &= \int_R \int_R \delta(w - w') f^{3\text{-D}}(u, v, w)\, dw\, dw' \\ &= \int_R f^{3\text{-D}}(u, v, w)\, dw. \end{aligned} \tag{11}$$

Combining eq. (11) with eqs (8) and (9), we obtain

$$f_g(u, v) = \int_R C_\rho^2 \frac{w^2}{|\mathbf{k}|^4} f_\rho(\mathbf{k})\, dw, \tag{12}$$

$$f_T(u, v) = \int_R C_\chi^2 \frac{w^4}{|\mathbf{k}|^4} f_\chi(\mathbf{k})\, dw, \tag{13}$$

relating the 2-D spectral density of the gravity and magnetic fields in a horizontal observation plane at $z=0$ to the spectral density of their respective sources.

Scaling sources

To assume a scaling source distribution with isotropic scaling exponent β means to assume that the 3-D spectral density of the source parameter has the form

$$f(u, v, w) = C_{\text{scale}} (\sqrt{u^2 + v^2 + w^2})^{-\beta}, \tag{14}$$

where C_{scale} is a constant indicating the intensity of the source variations.

Combining eqs (12) and (13) with eq. (14), we can derive the spectral density of the gravity and magnetic fields in a horizontal observation plane by solving the following integrals, as described in detail by Maus & Dimri (1994):

$$f_g(u, v) = C_\rho^2 C_{\text{scale}} \int_R \frac{w^2}{|\mathbf{k}|^4} (\sqrt{u^2 + v^2 + w^2})^{-\beta}\, dw$$

$$= C_g s^{-(\beta+1)}, \tag{15}$$

$$f_T(u, v) = C_\chi^2 C_{\text{scale}} \int_R \frac{w^4}{|\mathbf{k}|^4} (\sqrt{u^2 + v^2 + w^2})^{-\beta}\, dw$$

$$= C_T s^{-(\beta-1)}, \tag{16}$$

where C_g and C_T are constants and $s^2 = u^2 + v^2$.

It is interesting to note that the 2-D field in a horizontal observation plane caused by isotropic scaling sources is again scaling. However, in the case of magnetic data this is only valid for a field which has been reduced to the pole.

Limitations

By assuming a scaling source distribution in the form of eq. (14) the following two problems arise.

(1) The integral over the spectral density of eq. (14) is infinite for any β. Hence, this is the spectral density of a 3-D random field with infinite variance, which is incompatible with the fact that there are definite minimum and maximum possible values for the density and the susceptibility in the lithosphere. Therefore, we have to assume that the spectral densities of all the parameters regarded here fulfil eq. (14) only in a limited band of wavenumbers. Without this restriction, the random fields would not be homogeneous and could not be written as Fourier–Stieltjes integrals.

(2) Eq. (14) is the spectral density of a *full-space* of scaling sources, whereas our model is a *half-space* of scaling sources. We presume that the spectral density of a potential field on the surface of a half-space of scaling sources is identical to the spectral density given by (15) and (16) for the fields caused by a full-space of scaling sources, except for a constant factor. Although we have verified this assumption on synthetic data, we have not been able to give a mathematical proof, since we find it difficult to express the concept of a half-space in the Fourier–Stieltjes formalism.

Continuing the field upwards into the observation plane

To complete our model, we still have to continue the field upwards from the surface of the half-space to the observation plane. This is achieved by multiplying the spectral densities by $\exp(-2ts)$. Thus, we arrive at the following three-parameter model (C, t, γ) for the power spectral density of the field in the observation plane:

$$P_{\text{model}}(s) = C \exp(-2ts) s^{-\gamma}, \tag{17}$$

where P_{model} is the model power spectrum for gravity data $(\gamma = \beta + 1)$, or magnetic data reduced to the pole $(\gamma = \beta - 1)$; C is a constant dependent on the intensity of the anomalous source distribution and the units of measurement; t is the distance between the observation plane and the top of the postulated half-space of sources; s is the absolute value of the 2-D wavevector; β is the 3-D isotropic scaling exponent of the source distribution; and γ is the 2-D scaling exponent of the potential field directly above the sources. Eq. (17) for the magnetic field is similar to the relationship derived by Pilkington & Todoeschuck (1993) using a formula of Naidu (1968).

It should be mentioned here that Spector and Grant's approach implicitly assumes the power spectral density of the 2-D potential field to be constant at source level. This corresponds to the special case of eq. (17) with $\gamma = 0$, whereas realistic values of the scaling exponent for the magnetic field at source level are around $\gamma \approx 3$ (Gregotski *et al.* 1991).

APPLICATIONS

To confirm the above relationships, we first compare the power spectrum of synthetic magnetic data with the model power spectrum defined by eq. (17). Then we study three examples of power spectra from real gravity and aeromagnetic data. To fit the model power spectrum to the observed power spectra, we take the logarithm of eq. (17) and find the optimum parameter triplet $[\ln(C), t, \gamma]$ using the L_1-norm. Whenever we refer to a best fit, we mean that the misfit function between the model and the observed power spectrum has a minimum in the least absolute deviation (LAD) sense (Dimri 1992).

Synthetic data

A grid of $64 \times 64 \times 64$ cells is utilized to model the source distribution and a matrix of 64×64 pixels is used in the observation plane. We generate the source distribution in the wavenumber domain, using the definition of the 3-D Fourier–Stieltjes integral, and then transform the grid to the space domain by fast Fourier transform (FFT). The complex grid cells in the wavenumber domain correspond to the random measure $Z(d\mathbf{k})$. Thus, they have to fulfill the properties (1–3) mentioned above for eq. (1). In particular, they have to have zero mean, be statistically independent and their expected absolute value has to fulfill eq. (2). The imaginary part of the grid in the space domain has to be zero throughout, since the density and susceptibility are real functions. Therefore, when filling the grid in the wavenumber domain, certain rules have to be observed to ensure that the imaginary part of the grid in the space domain will be zero after Fourier transforming the grid.

Let us consider the following example. A susceptibility distribution with scaling exponent $\beta = 4$ is generated in the wavenumber domain. Every grid cell is to represent a volume of $500 \times 500 \times 500\ m^3$. One observation plane is situated on the surface of the grid and another 1 km above the grid, i.e. 0.25 and 1.25 km above the centre of the upper layer of grid cells. The synthetic data matrix in the observation plane for a vertical normal field is generated using the well-known formula for magnetic dipoles. After making the matrix periodic and transforming to the wavenumber domain by FFT, the power spectrum is obtained as the square of the complex Fourier coefficients. The radially averaged logarithmic power spectra of the synthetic data are shown in Fig. 1. For magnetic data, we expect a scaling exponent of $\gamma = \beta - 1$. The curves indicate the theoretical power spectra (17) for $t = 0$ km and $t = 1$ km with $\gamma = 3$.

Gravity data

Fig. 2 shows a power spectrum estimated by Pawlowski (1994) from a 120 km × 120 km gravity survey of the Paradox Basin Region in south-eastern Utah. The geology of the area is described briefly by Hildenbrand & Kucks (1983). More detailed information can be found in the Geological Atlas of the Rocky Mountain Region, published in 1972 by the Rocky Mountain Association of Geologists. Outcropping Precambrian basement with highly deformed metamorphic and igneous rocks is found in the north-east of the survey area as part of the Uncompahgre Uplift. South-west of the Uncompahgre front, overlying Precambrian basement, are Palaeozoic carbonates, clastics and evaporites followed by Mesozoic marine sandstones, shales and continental red beds with a maximum aggregate thickness of 7–8 km. High laccolithic mountains composed of diorite porphyry were formed during Late Cretaceous times. In addition to these igneous intrusions, the sedimentary layers are disturbed by prominent salt domes and anticlines.

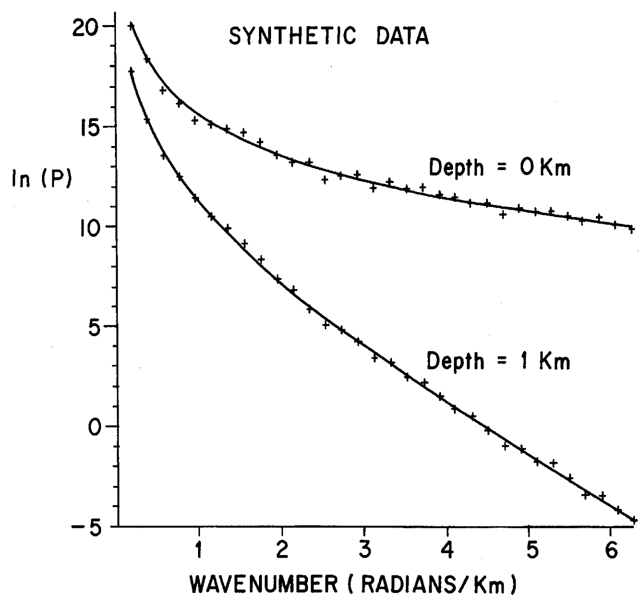

Figure 1. Radially averaged logarithmic power spectra of synthetic magnetic data generated for observation planes 1 km above and directly above a susceptibility distribution with scaling exponent $\beta = 4$. The curves give the theoretical power spectra for these configurations.

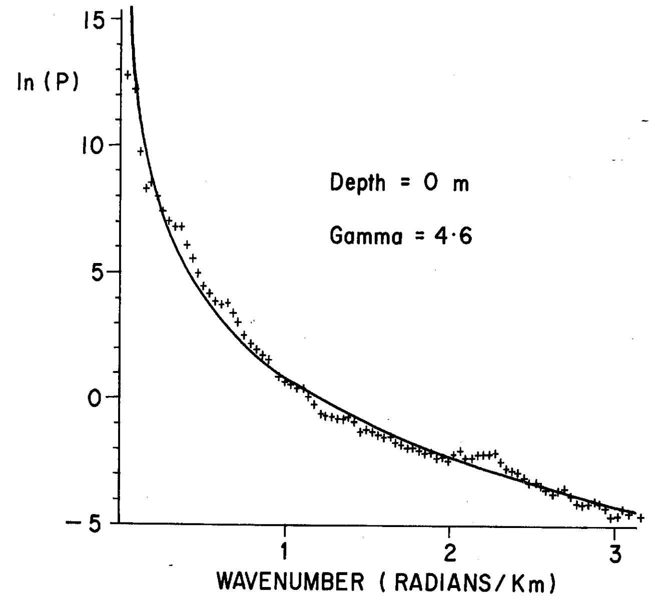

Figure 2. Radially averaged power spectrum of gravity data of the Paradox Basin Salt Anticline Region (after Pawlowski 1994). The author had estimated source depths of 5 and 54 km from the slope of the power spectrum. However, a model half-space with its top at surface level [$\ln(C) = 0.8$, $t = 0$, $\beta = 3.6$] explains the shape of the power spectrum quite well.

Pawlowski (1994) derived depth values of 5 and 54 km by the Spector and Grant method from the power spectrum of the Paradox Basin gravity data. These depth values were then utilized to separate the effects caused by shallow and deep-seated sources by Wiener filtering, assuming that long- and short-wavelength anomalies originate from deep-seated and shallow sources, respectively.

Comparing the power spectrum of the measured data with the model power spectrum defined by eq. (17), we obtain the misfit function displayed as a 2-D cross-section in Fig. 3. The best fit is found for $\ln(C) = 0.93$, $\gamma = 4.5$ and a source depth of 54 m, which is almost negligible considering the size of the survey area. The optimum model power spectrum for a fixed depth of $t = 0$ m is shown as a solid line in Fig. 2.

Using eq. (15), we conclude that the density variations caused by the various structures in and around the Paradox Basin are scaling with $\beta = 3.6$. Further information may not be present in this power spectrum.

Aeromagnetic data of a shield volcanic area

Hildenbrand *et al.* (1993) analysed power spectra of aeromagnetic data from the Island of Hawaii, which they interpreted by the Spector and Grant method as a four-layer model, because four lines were required in order to model the power spectra properly. The thickness of the first layer was found to be in the range of 0.8 to 1.8 km throughout the island. The second layer, with an average thickness of 1.5 km, was only found in certain areas. The deepest magnetic boundary (between the third and fourth layers) was found at 9 km below

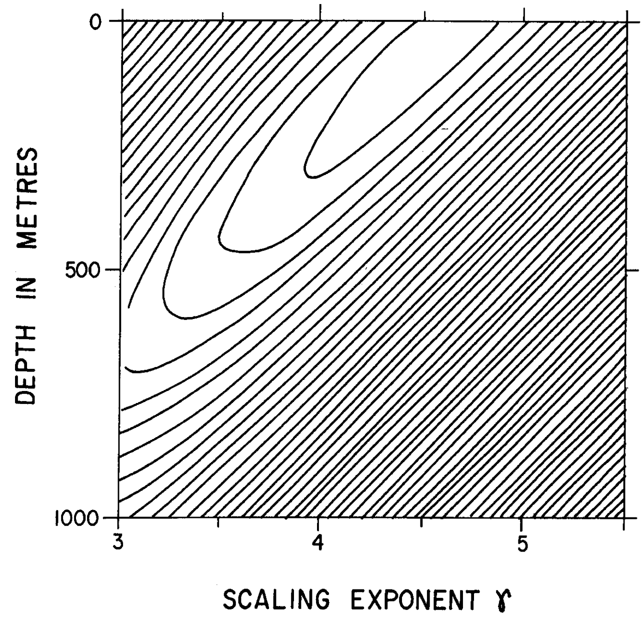

Figure 3. Misfit of the model power spectrum defined by eq. (17) regarding the power spectrum of Fig. 2 for different combinations of γ and t. The value of C has been optimized for each combination. Contour interval is 10 per cent of the minimum misfit.

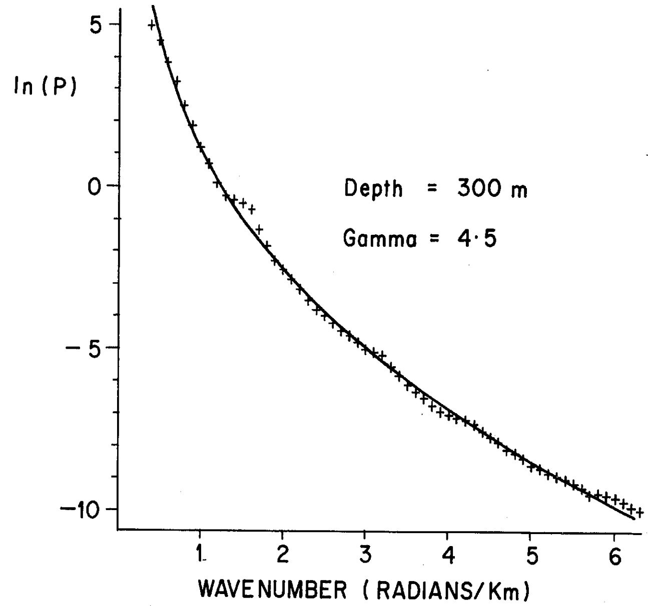

Figure 5. Data of Fig. 4 together with the model power spectrum for $t = 300$ m (the survey terrain clearance), $\ln(C) = -1.8$ and a susceptibility distribution with $\beta = \gamma + 1 = 5.5$.

sea-level, agreeing with the depth of the oceanic crust as determined from seismic data.

We will now reinterpret the power spectrum which Hildenbrand *et al.* gave in their publication and which is reproduced here in Fig. 4. Fig. 5 shows the data of Fig. 4, together with the model power spectrum for $t = 300$ m (the survey terrain clearance), $\ln(C) = -1.8$ and $\gamma = 4.5$. However, an optimum fit is achieved for $t = 243$ m, $\ln(C) = -2.1$ and $C = 4.8$. This is a deviation from the true survey terrain clearance of 20 per cent. The misfit function for different combinations of γ and the depth to source is displayed in Fig. 6. A crust consisting entirely of mafic, effusive material is

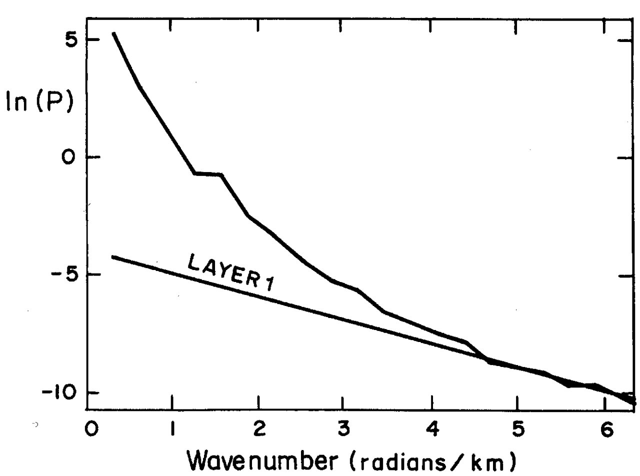

Figure 4. Radially averaged power spectrum of aeromagnetic data of the Island of Hawaii in semi-logarithmic scale with the depth of the first layer derived by the Spector and Grant method (after Hildenbrand *et al.* 1993).

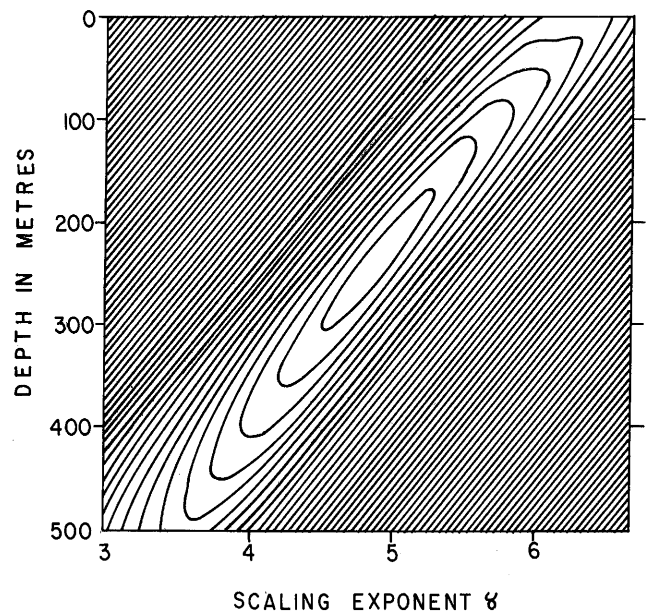

Figure 6. Misfit of the model power spectrum defined by eq. (17) regarding the power spectrum of Fig. 4 for various combinations of γ and t. The value of C has been optimized for each combination. Contour interval is 20 per cent of the minimum misfit.

the perfect example of a half-space with homogeneous statistical properties of the magnetization. The only depth information contained in this power spectrum is the depth to the surface of this half-space, i.e. the survey terrain clearance.

The scaling exponent $\gamma = 4.5$ of the field at surface level is high compared with the average value of $\gamma \approx 3$ derived by Gregotski *et al.* (1991) from aeromagnetic surveys of the North American continent. A high scaling exponent indicates a long-range dependence of the susceptibility distribution. This could be explained by the large lateral extent of high-temperature lava flows leading to correlated susceptibilities over considerable distances. The power spectrum of Fig. 4 was derived from a 17 km × 17 km area close to Mount Kilauea, the youngest of the five volcanoes on the island. It would be interesting to compare the scaling exponents of different areas to see whether any correlation with the age of the lava can be found.

Aeromagnetic data of a sedimentary basin

In the previous two examples we studied areas with outcropping source anomalies. Consequently, the inversion yielded the survey terrain clearance as optimum depth to source. Depth values other than the survey terrain clearance can only be obtained in a geological setup with a source-free top layer. Such a setup is studied in the following example.

A power spectrum of aeromagnetic data of the Athabaska sedimentary basin in Saskatchewan, Canada was derived and studied by Pilkington *et al.* (1994). The flight altitude of the survey was 300 m, and the depth to the basement, estimated from seismic refraction surveys and modelling of individual magnetic anomalies, is approximately 1400 m. Therefore, a reliable method should derive a depth value of about 1700 m from this power spectrum. According to Pilkington *et al.*, assuming a white magnetization distribution leads to a depth estimate of approximately 2400 m. For various aeromagnetic surveys of the North American continent, Gregotski *et al.* (1991) found scaling exponents of approximately $\gamma \approx 3$. Using this *a priori* information, Pilkington *et al.* adjusted the power spectrum by a scaling exponent of $\gamma = 3$ and found that the depth estimate obtained from the adjusted power spectrum was compatible with a depth to source of 1700 m. This is an interesting result, which will be elaborated on in the following.

The fit of the model power spectrum defined by eq. (17) for various scaling exponents is shown in Fig. 7. For a scaling exponent of $\gamma = 0$, corresponding to the Spector and Grant method, we find the best fit for a source depth of 3.6 km (using only the power of the first 20 wavenumbers), and for $\gamma = 3$ (using the power of the first 40 wavenumbers) we obtain a source depth of 1 km. An even better fit is found for a depth equal to the flight altitude, because the tail of the observed power spectrum is whiter (less steep) than it should be for a depth to source of 1 km (see Fig. 1). Hence, this power spectrum again seems to carry no other depth information than the flight altitude of the magnetometer.

However, Pilkington *et al.* (1994) have given a second power spectrum of an area immediately adjacent to the basin, with outcropping basement. The two power spectra are displayed together in Fig. 8. For power spectrum (b), we know that the depth to source is equal to the flight altitude. Under the constraint of $t = 300$ m, an optimum fit of the model power spectrum is found for $\ln(C) = 2.67$ and $\gamma = 2.2$. Let us now assume that in both areas the magnetic field caused by the basement has identical statistical properties. Then we can downward continue the model power spectrum that fitted spectrum (b) until it matches power spectrum (a) at low wavenumbers. This procedure, which is demonstrated in Fig. 8, yields a depth of 1700 ± 200 m, which is correct. The white tail of the power spectrum, however, remains unexplained. It could be caused by high-frequency noise, a non-negligible magnetization of the sediments, or by a bias of the power spectrum estimator towards higher powers at high wavenumbers.

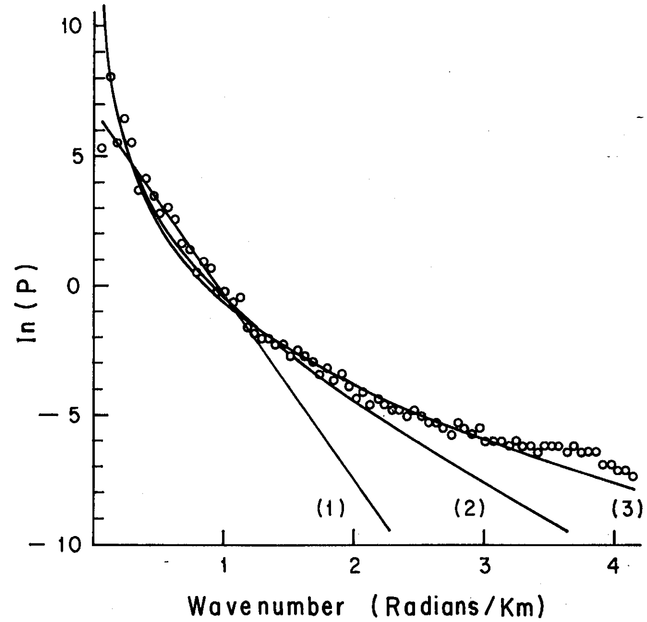

Figure 7. Power spectrum of aeromagnetic data of a sedimentary basin with an approximate depth of 1400 m (data from Pilkington *et al.* 1994). The survey was flown with a flight altitude of 300 m. Curve (1) gives the best fit for $\gamma = 0$ (Spector and Grant method) resulting in an estimated depth of 3.6 km. Curve (2), for $\gamma = 3$, leads to a depth estimate of 1 km. An even better fit is achieved by curve (3) for $\gamma = 3.8$ and a model depth equivalent to the survey terrain clearance.

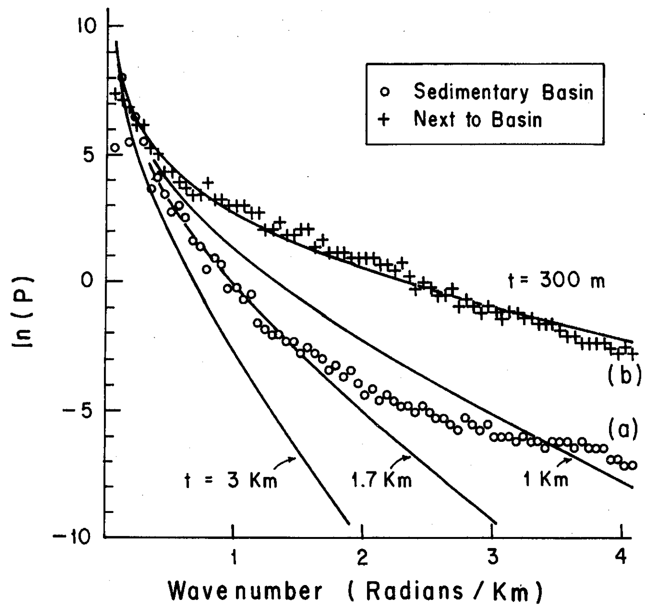

Figure 8. Power spectrum of Fig. 7 labelled (a), together with the power spectrum for an area with outcropping basement, labelled (b). Under the constraint t = flight altitude = 300 m, an optimum fit of the model power spectrum to power spectrum (b) was found for $\gamma = 2.2$ and $\ln(C) = 2.67$. The curves labelled $t = 1$ km, $t = 1.7$ km, and $t = 3$ km show the model power spectrum for the same values of C and γ, but for different depths.

CONCLUSIONS

(1) The assumption of a white-noise field at source level is unrealistic and leads to arbitrary depth estimates from the power spectrum of potential field data.

(2) Self-similar (scaling) random fields provide realistic models for the density and susceptibility distributions in the Earth's crust. A half-space model of isotropic scaling sources leads to a model power spectrum with three parameters, namely the depth to source t, the intensity C of the field, and the scaling exponent γ of the field.

(3) Power spectra of surveys over outcropping sources are explained well by a half-space model with its top at surface level. Generally, the only depth information contained in such power spectra appears to be the survey terrain clearance.

(4) Basin depth estimation from the power spectrum is complicated by a trade-off between the scaling exponent γ and the depth to source t.

(5) The theoretical power spectrum for a basin with source-free sediments falls off rapidly at high wavenumbers, whereas the power spectra of real data tend to have flat tails. Whatever the cause for this discrepancy may be, it is probably the main obstacle to basin depth estimation from the power spectrum of potential field data.

ACKNOWLEDGMENTS

We thank H. K. Gupta, Director NGRI, for encouragement and permission to publish this work. Fruitful discussions with S. K. Verma are gratefully acknowledged. This paper has benefited substantially from suggestions made by G. Müller, DGG editor, and comments of the two anonymous reviewers.

REFERENCES

Blakely, R.J., 1988. Curie temperature isotherm analysis and tectonic implications of aeromagnetic data from Nevada, *J. geophys. Res.*, **93,** 11 817–11 832.

Bosum, W., Damaske, D., Roland, N.W., Behrendt, J. & Saltus, R., 1989. The Ganovex IV Victoria Land/Ross Sea aeromagnetic survey: Interpretation of anomalies, *Geologisches Jahrbuch,* **E 38,** 153–230.

Connard, G., Couch, R. & Gemperle, M., 1983. Analysis of aeromagnetic measurements from the Cascade Range in central Oregon, *Geophysics,* **48,** 376–390.

Cowan, D.R. & Cowan, S., 1993. Separation filtering applied to aeromagnetic data, *Exploration Geophysics,* **24,** 429–436.

d'Arnaud Gerkens, J.C., 1989. *Foundation of exploration geophysics,* Elsevier, Amsterdam.

Dimri, V.P., 1992. *Deconvolution and inverse theory,* Elsevier, Amsterdam.

Garcia-Abdeslem, J. & Ness, G.E., 1994. Inversion of the power spectrum from magnetic anomalies, *Geophysics,* **59,** 391–401.

Gregotski, M.E., Jensen, O.G. & Arkani-Hamed, J., 1991. Fractal stochastic modeling of aeromagnetic data, *Geophysics,* **56,** 1706–1715.

Hahn, A., Kind, E.G. & Mishra, D.C., 1976. Depth estimation of magnetic sources by means of Fourier amplitude spectra, *Geophys. Prospect.,* **24,** 287–308.

Hildenbrand, T.G. & Kucks, R.P., 1983. Regional magnetic and gravity features of the Gibson Dome area and surrounding region, Paradox Basin, Utah: A preliminary report, *Open-File Report,* **83–359,** US Geological Survey.

Hildenbrand, T.G., Rosenbaum, J.G. & Kauahikaua, J.P., 1993. Aeromagnetic study of the Island of Hawaii, *J. geophys. Res.,* **98,** 4099–4119.

Jacobsen, B.H., 1987. A case for upward continuation as a standard separation filter for potential field maps, *Geophysics,* **52,** 1138–1148.

Mandelbrot, B.B., 1983. *The fractal geometry of nature,* W.H. Freeman, New York, NY.

Maus, S. & Dimri, V.P., 1994. Scaling properties of potential fields due to scaling sources, *Geophys. Res. Lett.,* **21,** 891–894.

Militzer, H. & Weber, F., 1984. *Angewandte Geophysik,* Vol. 1, Akademie-Verlag, Berlin.

Naidu, P.S., 1968. Spectrum of the potential field due to randomly distributed sources, *Geophysics,* **33,** 337–345.

Naidu, P.S., 1972. Maximum likelihood (ML) estimation of depth from the spectrum of aeromagnetic fields, *Pure appl. Geophys.,* **95,** 141–149.

Ofoegbu, C.O. & Hein, K., 1991. Analysis of magnetic data over part of the Younger Granite Province of Nigeria, *Pure appl. Geophys.,* **136,** 173–189.

Okubo, Y. & Matsunaga, T., 1994. Curie point depth in northeast Japan and its correlation with regional thermal structure and seismicity, *J. geophys. Res.,* **99,** 22 363–22 371.

Pawlowski, R.S., 1994. Green's equivalent-layer concept in gravity band-pass filter design, *Geophysics,* **59,** 69–76.

Pawlowski, R.S., 1995. Preferential continuation for potential-field anomaly enhancement, *Geophysics,* **60,** 390–398.

Pedersen, L.B., 1991. Relations between potential fields and some equivalent sources, *Geophysics,* **56,** 961–971.

Pilkington, M. & Todoeschuck, J.P., 1990. Stochastic inversion for scaling geology, *Geophys. J. Int.,* **102,** 205–217.

Pilkington, M. & Todoeschuck, J.P. 1993. Fractal magnetization of continental crust, *Geophys. Res. Lett.,* **20,** 627–630.

Pilkington, M. & Todoeschuck, J.P., 1995. Scaling nature of crustal susceptibilities, *Geophys. Res. Lett.,* **22,** 779–782.

Pilkington, M., Gregotski, M.E. & Todoeschuck, J.P., 1994. Using fractal crustal magnetization models in magnetic interpretation, *Geophys. Prospect.,* **42,** 677–692.

Shuey, R.T., Schellinger, D.K., Tripp, A.C. & Alley, L.B., 1977. Curie depth determination from aeromagnetic spectra, *Geophys. J. R. astr. Soc.,* **50,** 75–101.

Spector, A. & Grant, F.S., 1970. Statistical models for interpreting aeromagnetic data, *Geophysics,* **35,** 293–302.

Turcotte, D.L., 1992. *Fractals and chaos in geology and geophysics,* University Press, Cambridge.

Whaler, K.A., 1994. Downward continuation of Magsat lithospheric anomalies to the Earth's surface, *Geophys. J. Int.,* **116,** 267–278.

Yaglom, A.M., 1986. *Correlation theory of stationary and related random functions,* Vol. 1, Springer-Verlag, New York, NY.